Preliminary NGA-West 2 models for ground-motion directionality

S.K. Shahi & J.W. Baker
Stanford University, Stanford, CA, USA

SUMMARY:
The NGA-West 2 program, coordinated by the Pacific Earthquake Engineering Research Center (PEER), is a major effort to produce refined models for predicting ground motion response spectra. This paper presents new models for ground-motion directionality developed as part of that project. Using a database of recorded strong ground motions, empirical models have been developed for a variety of quantities related to direction-dependent spectra. Predictions are available for the maximum spectral acceleration observed in any orientation of two-component horizontal ground-motion shaking ("$Sa_{RotD100}$"). This model is formulated as a multiplier factor to be coupled with the NGA West 2 models that predict the median spectral accelerations over all orientations (Sa_{RotD50}). A model has been developed for the distribution of orientations of the $Sa_{RotD100}$ value relative to the fault. Discussion is provided as to how these results can be applied to practical seismic hazard analysis and earthquake engineering problems.

Keywords: ground-motion model, NGA-West 2, Directionality

1. INTRODUCTION

Structures designed to resist seismic loads are generally designed considering the ground motion in the horizontal plane. However the acceleration response spectrum, which is the intensity-measure (IM) used for design, is defined as the maximum response of a single degree of freedom system at different periods when excited by a single component of the ground motion. So, even though two dimensional ground motions are considered for design, the intensity-measure is defined to represent single component of the ground motion. Various methods have been proposed in past to compute an intensity-measure representative of the two-dimensional horizontal ground motion. These methods include using the geometric mean of the acceleration response spectra computed using two orthogonal components of ground motion, using the median or maximum value of response spectra over all orientations at each period etc. (Boore et. al 2006, Boore 2010)

The NGA-West 2 program, coordinated by Pacific Earthquake Engineering Research Center (PEER), will produce refined models for predicting the median ground-motion response spectra of a ground motion when rotated over all horizontal orientations; this is referred to as the Sa_{RotD50} spectrum. It is known that ground-motion intensity is not uniform in all orientations. In some cases ground motions can be polarized and intensity in one orientation can be significantly stronger than in other orientations (Huang et al., 2008). This phenomenon is often referred as "directionality" of ground motion. Many engineers believe that due to ground motion directionality, the maximum spectral acceleration over all orientations ($Sa_{RotD100}$) is a more meaningful intensity measure than Sa_{RotD50} for structural design (NEHRP, 2009). The NEHRP (2009) provisions use $Sa_{RotD100}$ as the ground-motion intensity measure for design. Thus, different definitions of ground-motion intensity will be used to build ground-motion models (Sa_{RotD50}) and for structural design ($Sa_{RotD100}$). The need to use a consistent intensity-measure throughout the design process (e.g., Baker and Cornell, 2006, Beyer and Bommer, 2006) requires models to convert between the two definitions of IM. Additionally, there is interest in whether the $Sa_{RotD100}$ is observed in random orientations or has preferential alignment in, for example, near-fault ground motions. This also has potentially important implications for structural design.

Several researchers have modeled the ratio of different intensity-measures which can be used as a multiplicative factor to convert between them (e.g., Beyer and Bommer 2006, Watson-Lamprey and Boore 2007, Huang et al. 2008, 2010). Most of these studies used subsets of the NGA database (Chiou et al. 2008) and focused on the ratios involving the older $Sa_{GMRotI50}$ definition of response spectrum. In this study we use over 3000 ground motions from the expanded NGA-West 2 database to build empirical models for the ratio of $Sa_{RotD100}$ to Sa_{RotD50} and the probability distribution of orientations in which the $Sa_{RotD100}$ is observed. The model predicting the ratio of $Sa_{RotD100}$ to Sa_{RotD50} can be used as a multiplicative factor that when used with the upcoming NGA-West 2 ground-motion models can predict the $Sa_{RotD100}$ at a site. The proposed models are compared with older models and differences are discussed.

2. GROUND-MOTION INTENSITY AND DIRECTIONALITY

Several methods have been used in the past to construct a response spectrum to represent the intensity of a two dimensional horizontal ground motion. Early efforts to account for the two-dimensional intensity of ground motion used the geometric mean of response spectra computed using two orthogonal components of the ground motion (sometimes referred as Sa_{GM}). Generally the two orientations in which the ground motion was recorded ("as-recorded orientations") or the fault-normal and parallel orientations are used for computing Sa_{GM}. Using the as-recorded orientations of the ground motion makes the ground-motion intensity dependent on the orientation of the recording instrument which is often arbitrary. The fault-normal and parallel orientations are important for near-fault sites as near-fault effects are generally observed in these orientations (directivity in fault-normal, fling in fault-parallel for strike-slip earthquakes), but these orientations have no special significance for sites located far from the fault.

In order to remove the dependence of IM on arbitrarily selected orientations, Boore et al. (2006) introduced $Sa_{GMRotDnn}$ and $Sa_{GMRotInn}$ intensity measures, which are orientation independent definitions of ground-motion intensity. $Sa_{GMRotDnn}$ is defined as the nn^{th} percentile of the set of all possible response spectra computed by taking geometric means of two orthogonal response spectra at a specified period. The $Sa_{GMRotDnn}$ spectrum may use the geometric means from different orientations at different periods. An intensity measure that is constructed using spectral acceleration from different orientations at each period does not represent any particular observation of two components of the ground motion. $Sa_{GMRotInn}$ fixes this by defining the intensity measure as the geometric mean of response spectra at the orientation most representative of the $Sa_{GMRotDnn}$ spectrum across a range of periods. This definition uses the geometric mean of two orthogonal spectra which were observed at the site. The 2008 version of NGA ground-motion models were developed to predict the $Sa_{GMRotI50}$ at a site.

Though the $Sa_{GMRotInn}$ spectrum captures information from multiple orientations and is orientation and period independent, it is difficult to compute. So, a new IM called Sa_{RotDnn} was proposed by Boore (2010), which is defined as the nn^{th} percentile of the spectral acceleration at each period over all orientations. Like $Sa_{GMRotDnn}$, the nn^{th} percentile spectral acceleration at each period may occur in different orientations. Despite this property, the orientation independent and simple definition has made Sa_{RotDnn} a popular ground-motion intensity-measure. The new ground-motion models being developed as part of the NGA-West 2 project will predict Sa_{RotD50} values.

In general, constructing a single response spectrum to represent two-dimensional ground-motion intensity involves reducing information in two dimensions to one, which results in loss of information. Different definitions of ground-motion intensity capture different pieces of this information and thus may be appropriate for different tasks. If the ground-motion is unpolarized then it will have equal intensity in all orientations (i.e., no directionality). In this no-polarization case, illustrated in figure 1a, all definitions of ground-motion intensity will give the same result. Hence, the ratio of $Sa_{RotD100}$ to Sa_{RotD50} will always be 1 in this unpolarized case. However, if the ground motion is strongly polarized,

as illustrated in figure 1b, the various definitions of Sa will differ significantly in value. In this case, different definitions of IM will give different results and the ratio of $Sa_{RotD100}$ to Sa_{RotD50} is 1.414. A real ground motion generally lies between these two extreme cases and the $Sa_{RotD100}$ to Sa_{RotD50} ratio lies between 1 and 1.414 as shown in figure 2. So the intensity of ground motion computed using Sa_{RotD50} or $Sa_{RotD100}$ can differ for various ground motions, with the difference ranging from 0 to 41% of the Sa_{RotD50} intensity.

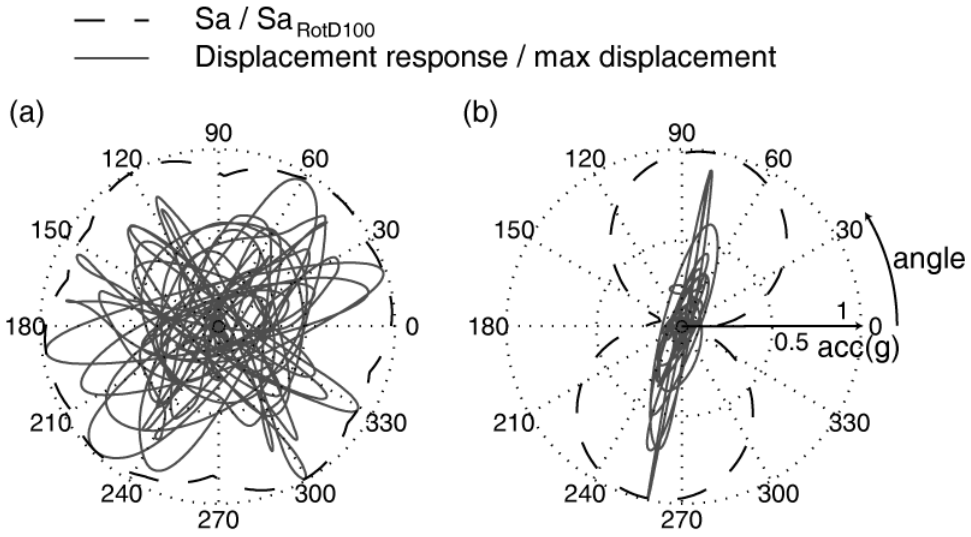

Figure 1. Displacement response trace (T = 1 sec) and spectral acceleration in all orientations (a) when ground motion is almost unpolarized (HWA031 recording from Chi-Chi-04, 1999 earthquake) and (b) when the ground motion is almost completely polarized (Gilroy Array#6 recording from Morgan Hill,1984 earthquake).

The polarization of ground motion is also referred as directionality of ground motion. It is the directionality of ground motions which causes discrepancy among different definitions of response spectrum and thus the models used to convert between different ground motion intensity-measures are referred to as directionality models in this paper.

3. RATIO OF $Sa_{RotD100}$ TO Sa_{RotD50}

As discussed earlier the NEHRP (2009) provisions recommend using $Sa_{RotD100}$ as the intensity-measure for design while the NGA-West 2 ground-motion models are being developed to predict Sa_{RotD50}. Models to convert between the two definitions are thus needed to allow the use of consistent definition of IM throughout the design process.

We computed the ratio of $Sa_{RotD100}$ to Sa_{RotD50} for each ground motion in the subset of NGA-West 2 database being used to develop the Abrahamson-Silva ground-motion model. The geometric mean of these ratios can be used as a multiplicative factor to convert Sa_{RotD50} intensity to $Sa_{RotD100}$ and its logarithm as an additive factor to convert $\ln Sa_{RotD50}$ to $\ln Sa_{RotD100}$. As ground-motion intensities are assumed to be log-normally distributed and the ground-motion models predict the natural log of intensity, the geometric mean of the ratios was preferred over arithmetic mean as shown in equations 3.1 to 3.3.

$$Sa_{RotD100} = \frac{Sa_{RotD100}}{Sa_{RotD50}} \cdot Sa_{RotD50} \tag{3.1}$$

$$\ln Sa_{RotD100} = \ln\left(\frac{Sa_{RotD100}}{Sa_{RotD50}}\right) + \ln Sa_{RotD50} \tag{3.2}$$

$$E(\ln Sa_{RotD100}) = E\left(\ln\left(\frac{Sa_{RotD100}}{Sa_{RotD50}}\right)\right) + E(\ln Sa_{RotD50}) \tag{3.3}$$

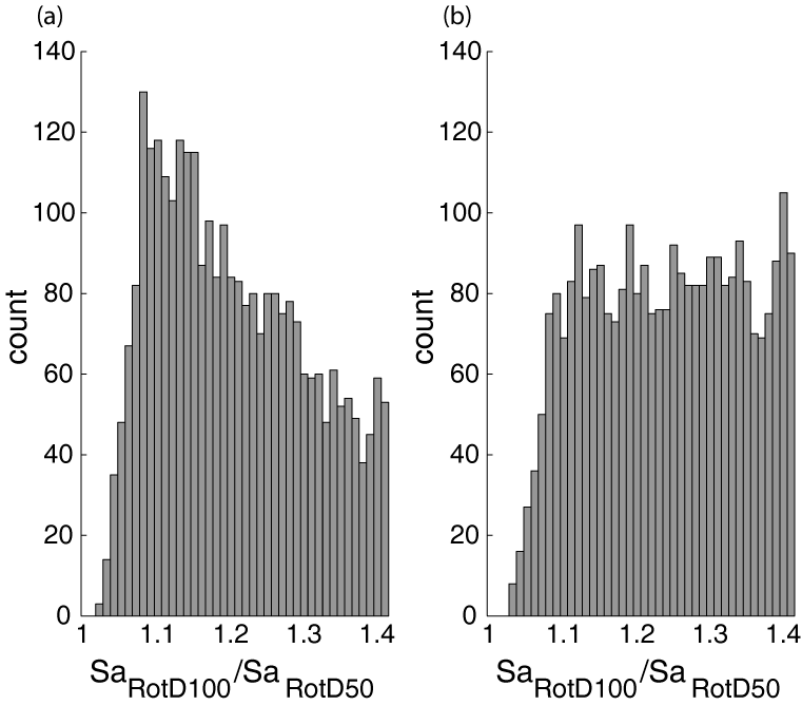

Figure 2. Histograms of observed $Sa_{RotD100}/Sa_{RotD50}$ ratios in the NGA-West 2 database for a) T = 0.2 sec and b) T = 1 sec.

The arithmetic mean of $\ln(Sa_{RotD100}/Sa_{RotD50})$ is used to estimate the $E(\ln(Sa_{RotD100}/Sa_{RotD50}))$ in equation 3.3. The exponential of the arithmetic mean of $\ln(Sa_{RotD100}/Sa_{RotD50})$ is the geometric mean of $Sa_{RotD100}/Sa_{RotD50}$. The empirically computed geometric mean of $Sa_{RotD100}/Sa_{RotD50}$ at different periods is shown in figure 3. Results computed using different subsets of the NGA West-2 database used to develop other ground-motion models were found to be consistent with each other.

Huang et al. (2008, 2010) reported that ground motion from Chi-Chi earthquake had a significant effect on the geometric mean of the ratio of observed $Sa_{RotD100}$ to $Sa_{GMRotI50}$ values predicted by ground-motion models, so they reported different sets of results for datasets with and without the Chi-Chi records. In this study we found that presence or absence of Chi-Chi records did not change the geometric mean of observed $Sa_{RotD100}$ to observed Sa_{RotD50} significantly. This indicates that the observed to observed ratio are more stable across different earthquake events compared to the observed to predicted ratio.

3.1. Comparison with other models

Several researchers have computed estimates for the ratio of $Sa_{RotD100}$ to $Sa_{GMRotI50}$ in past (e.g., Beyer and Bommer 2006, Watson-Lamprey and Boore 2007, Huang et al. 2008, 2010). In order to compare the older ratios of $Sa_{RotD100}$ to $Sa_{GMRotI50}$ with the $Sa_{RotD100}$ to Sa_{RotD50} ratios computed in this study, we used the factors proposed by Boore (2010) to convert the proposed $Sa_{RotD100}/Sa_{RotD50}$ ratios to $Sa_{RotD100}/Sa_{GMRotI50}$ ratios. Figure 4 compares our converted $Sa_{RotD100}$ to $Sa_{GMRotI50}$ ratios with previous results. Most of these models agree with each other in both the magnitude of the ratios and their trend with period. The one exception is the ratios proposed in NEHRP (2009) provisions.

The NEHRP (2009) $Sa_{RotD100}/Sa_{GMRotI50}$ ratios are based on the ratio of observed $Sa_{RotD100}$ values in recorded ground motions to the prediction of $Sa_{GMRotI50}$ by a ground-motion model. Modeling the ratio of an observed value to a predicted value, rather than the ratio of an observed value to an observed value, has some flaws. NGA models are carefully fitted to provide an unbiased estimate of ground-motion intensity from future earthquakes. However, the dataset used to fit the ground-motion models

is not an unbiased sample of earthquakes (e.g., there are many more ground motions from Chi-Chi, Taiwan earthquake in the NGA database compared to other earthquakes). Statistical techniques such as mixed-effects regression have been used to overcome these biases in the dataset while fitting the NGA ground-motion models. The ratios recommended by NEHRP (2009) provisions effectively readjust the NGA ground-motion models, which undoes careful calculations that go into building a ground-motion model. For example, a particular earthquake can produce higher average ground-motion intensities than the unbiased ground-motion model estimate due to random chance (any effect not accounted for by the ground-motion model can be modeled as random chance). The ratios of observed $Sa_{RotD100}$ to the predicted Sa_{RotD50} for such an earthquake will be higher than the ratio of observed $Sa_{RotD100}$ to observed Sa_{RotD50}, as the first ratio will also include the random earthquake effect (which is carefully removed by the mixed effects regression used to fit ground-motion models). Modeling $Sa_{RotD100}/Sa_{RotD50}$ as the ratio of observed $Sa_{RotD100}$ to observed Sa_{RotD50}, and using the prediction from a ground-motion model as an estimate for $E(\ln Sa_{RotD50})$ in equation 3.3 allows us to leverage the results from careful fitting of ground-motion models and gives us a better estimate of $Sa_{RotD100}$ from a future earthquake.

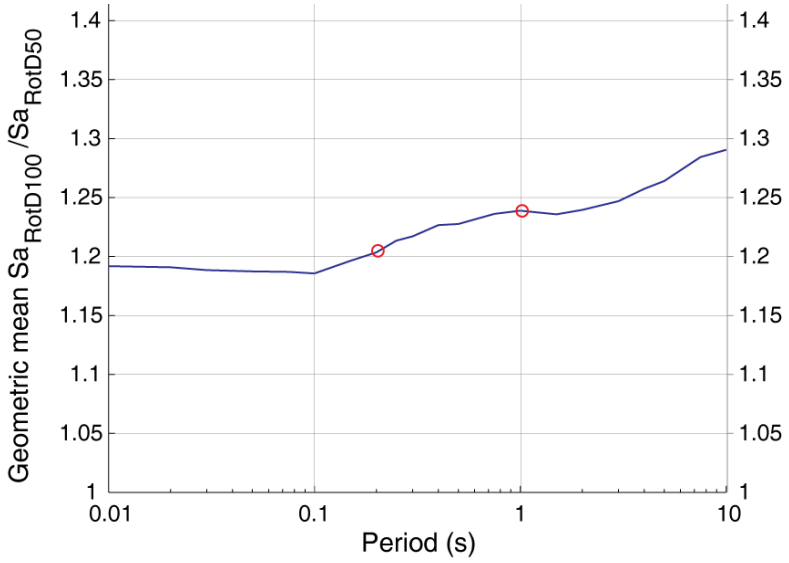

Figure 3. Geometric mean of the observed ratio of $Sa_{RotD100}$ to Sa_{RotD50} in NGA-West 2 database. The ratios for periods 0.2 sec and 1 sec are highlighted by circles.

3.2. Dependence of $Sa_{RotD100}/Sa_{RotD50}$ ratio on other parameters

Figures 2 and 3 showed that the geometric mean value of $Sa_{RotD100}/Sa_{RotD50}$ depends on spectral acceleration period. We also investigated its dependence on other seismological parameters. Figures 5 and 6 illustrate the dependence of $Sa_{RotD100}/Sa_{RotD50}$ at two periods on closest distance between the rupture and the site (R) and the earthquake magnitude (M) respectively. We studied the dependence of this ratio on other seismological parameters and fitted several regression models using variable selection techniques like forward selection, backward elimination etc. After examining the practical and statistical significance of different models, we decided to develop a model for $ln(Sa_{RotD100}/Sa_{RotD50})$ that was a linear function of R. Other parameters such as magnitude, directivity predictor terms, etc., had no appreciable predictive power. The linear model, shown in equation 3.4, contains a coefficient a_0 that varies with period and a coefficient a_1 that is constant for all periods and is estimated to be $-1.36\text{x}10^{-4}$.

$$E\left[\ln\left(\frac{Sa_{RotD100}}{Sa_{RotD50}}\right)\right] = a_0 + a_1 \cdot (R - 60) \tag{3.4}$$

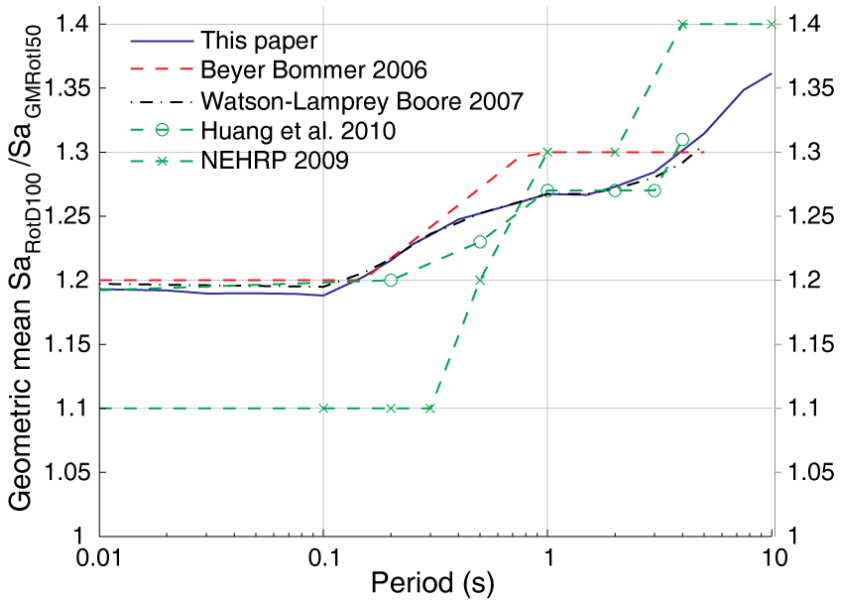

Figure 4. Comparison of various models for geometric mean $Sa_{RotD100}/Sa_{GMRotI50}$ ratios.

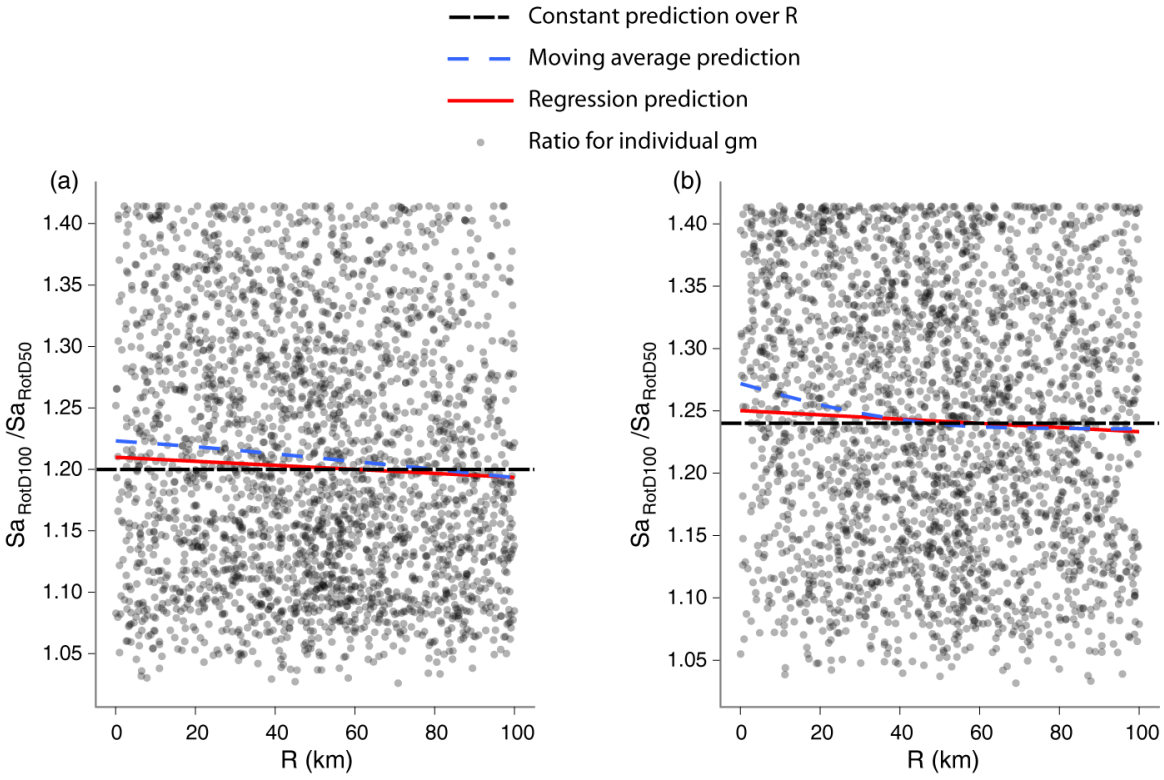

Figure 5. Regression and moving average predictions of $Sa_{RotD100}/Sa_{RotD50}$ with R for a) T = 0.2 sec, b) T = 1 sec.

As the difference between the results from using a distance dependent model or using a non-distance dependent model is small, we report both the geometric mean of the ratio of $Sa_{RotD100}$ and Sa_{RotD50} and the coefficient a_0 from equation 3.4 at different periods in table 3.1. Either of the two models can be used depending on the level of precision required. This view is echoed in the earlier study by Watson-Lamprey and Boore (2006), who noted slight distance, magnitude and radiation pattern dependence, but stated that "for most engineering applications the conversion factors independent of those

variables can be used." The results are reported at discrete set of periods and coefficients at other periods can be estimated by interpolating these results.

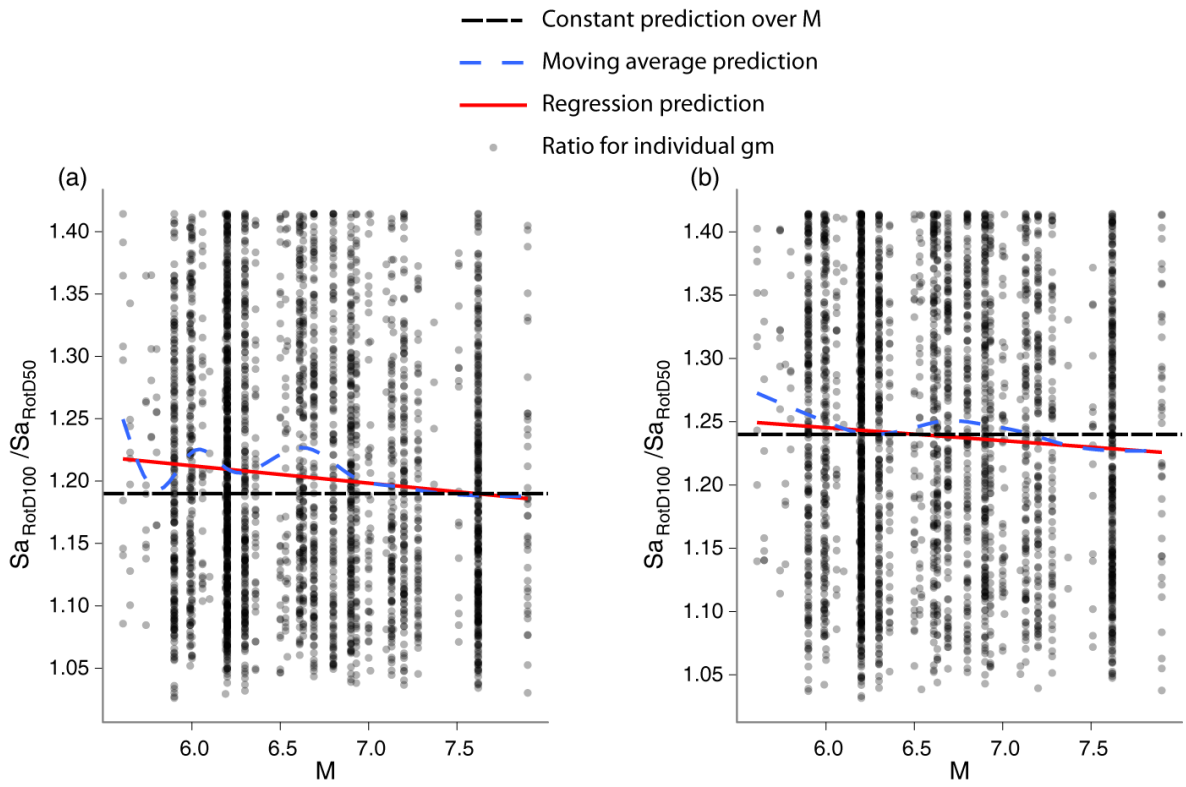

Figure 6 Regression and moving average predictions of $Sa_{RotD100}/Sa_{RotD50}$ with M for a) T = 0.2 sec and b) T = 1 sec.

Table 3.1. Geometric mean of $Sa_{RotD100}/Sa_{RotD50}$ and a_0 coefficients for equation 3.4

Period(s)	Geometric mean $Sa_{RotD100}/Sa_{RotD50}$	a_0 (i.e., ln(Geometric mean $Sa_{RotD100}/Sa_{RotD50}$))
0.01	1.19	0.174
0.02	1.19	0.174
0.03	1.19	0.174
0.05	1.19	0.174
0.075	1.19	0.174
0.1	1.19	0.174
0.15	1.20	0.182
0.2	1.20	0.182
0.25	1.21	0.191
0.3	1.22	0.199
0.4	1.23	0.207
0.5	1.23	0.207
0.75	1.24	0.215
1.0	1.24	0.215
1.5	1.24	0.215
2.0	1.24	0.215
3.0	1.25	0.223
4.0	1.25	0.223
5.0	1.26	0.231
7.5	1.28	0.247
10.0	1.29	0.255

4. ORIENTATION OF $Sa_{RotD100}$

Structural systems other than very simple ones (e.g., flag poles) generally have different resistance to seismic loads in different orientations. For these systems, the orientation in which the maximum intensity occurs is also important. We define the orientation of $Sa_{RotD100}$ as the minimum angle between the strike of the fault and the orientation of $Sa_{RotD100}$. This orientation, referred as α hereafter, ranges from 0 to 90 degrees where $\alpha = 0$ represents the strike-parallel orientation and $\alpha = 90$ represent the strike-normal orientation. Though these two orientations are not exactly the fault-parallel and normal orientations, they are often close to the fault-normal and fault-parallel orientation and in most cases can be taken as an approximation to these orientations.

To study these orientations, we computed α for each ground motion in our database at 21 periods, and then binned the data according to different seismological parameters and examined the distribution of α in each bin. Figure 7 shows distribution of α in different M and R bins. α is closer to strike-normal orientation ($\alpha = 90$) more often than to strike-parallel orientation ($\alpha = 0$) when the site is located within 5 km of the fault. On the other hand, when R is greater than 5 km, α is almost uniformly distributed. The magnitude bins do not seem to have any significant influence on the distribution of α.

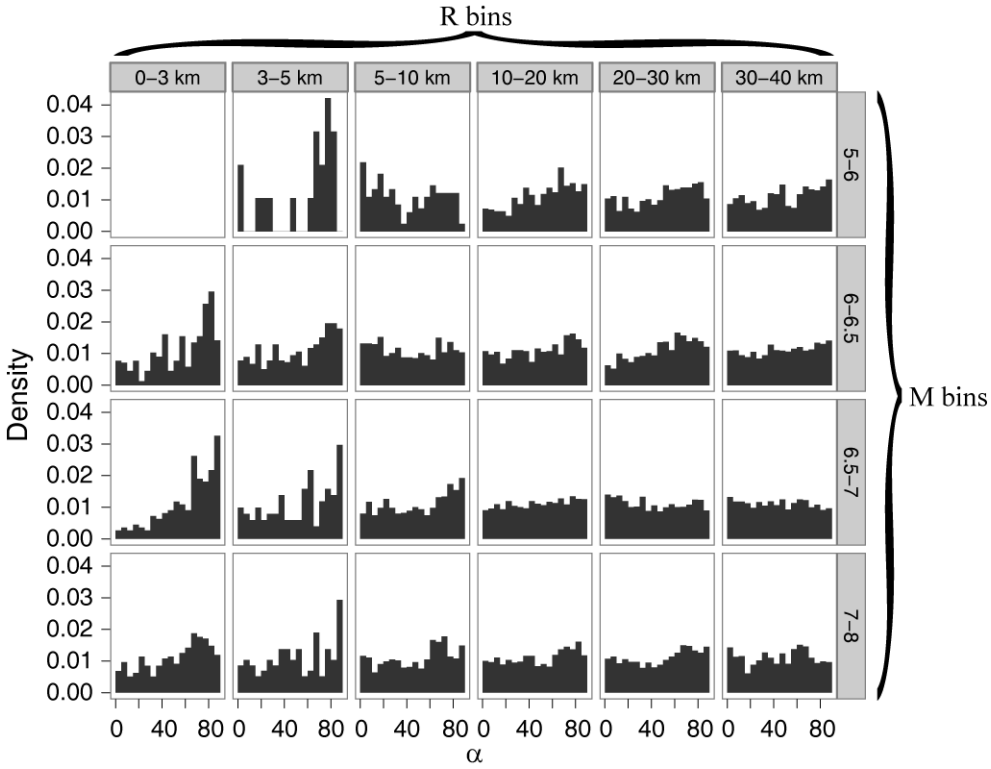

Figure 7. Probability density of α ($Sa_{RotD100}$ orientations) in different M, R bins

To examine the effect of period on $Sa_{RotD100}$ orientation (α), we binned all the data within 5 km of the fault by period. Histogram of α in different period bins is shown in figure 8. The distribution of α is nearly uniform for periods less than 1 sec, while orientations close to strike-normal are more frequent than strike-parallel for periods larger than 1 sec. Directivity effects observed at sites close to the fault can polarize the ground motion and cause stronger intensity in the fault-normal orientation than in the fault-parallel orientation at longer periods. This can explain the observation that α is uniformly distributed at low periods or large distances and is more frequently strike-normal for higher periods at sites close to the fault.

After examining histograms of α binned by several parameters we decided to model the distribution of α as uniform for sites when R is greater than 5 km or when the spectral-acceleration period under consideration is less than 1 second. For other cases (R < 5 km and $T \geq 1$ sec) the data was pooled and the distribution was modelled empirically by counting the number of α observed in 10 degree bins. This empirically computed distribution is presented in table 4.1 below.

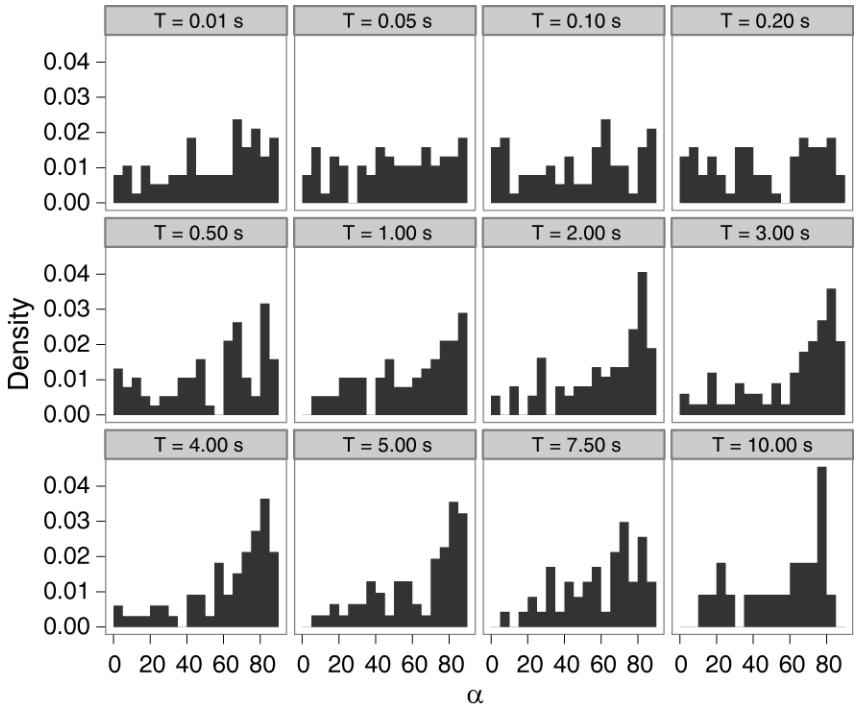

Figure 8. Probability density of α for sites with R < 5 km binned by Period (sec)

Table 4.1. Probability density of α for R < 5km and $T \geq 1$ sec

Orientations (degrees)	Probability
0-10	0.031
10-20	0.055
20-30	0.070
30-40	0.067
40-50	0.080
50-60	0.100
60-70	0.106
70-80	0.233
80-90	0.258

4. CONCLUSION

In this study, we examined different methods of representing the intensity of ground motion in the horizontal plane using a response spectrum which is a one dimensional representation of ground-motion intensity. We focused on two orientation-independent representations of the response spectrum: Sa_{RotD50} and $Sa_{RotD100}$. The new ground-motion models being developed as part of the NGA-West 2 project will predict the Sa_{RotD50} spectrum at a site due to a future earthquake, while the NEHRP (2009) provisions recommend using $Sa_{RotD100}$ for seismic design. We proposed a model to predict the ratio of $Sa_{RotD100}$ to Sa_{RotD50}, which can be used as a multiplicative factor with the Sa_{RotD50} predictions from the new NGA-West 2 ground-motion models to predict the $Sa_{RotD100}$ ground-motion intensity. The proposed model was compared and was found to be consistent with similar models built in the past, though the proposed model advances that earlier work by using a larger data set and utilizing the recently adopted Sa_{RotD50} definition instead of $Sa_{GMRotI50}$. The differences between the proposed model and corresponding NEHRP (2009) ratios were also explained.

Along with modelling the ratio of $Sa_{RotD100}$ to $Sa_{RotD50,}$ we also modelled the probability distribution of orientations in which the $Sa_{RotD100}$ intensity is observed relative to the strike of the fault. The orientations of $Sa_{RotD100}$ were observed to be uniformly distributed when the closest distance between the fault and the site was greater than 5 km or if the period under consideration was less than 1 sec. Only for the cases when the site was within 5 km of the fault and at periods greater than 1 sec, the orientation of $Sa_{RotD100}$ was more likely to be closer to the strike-normal than strike-parallel direction. Together these models can help solve a practical problem of converting between two important intensity-measures while helping deepen the understanding of the directionality of ground-motion by studying the distribution of orientations in which $Sa_{RotD100}$ occurs and dependence of $Sa_{RotD100}$ to Sa_{RotD50} ratio on different seismological parameters.

Planned future documentation of this work will include final refinements to the above models, as well as additional relevant information such as standard deviations of $Sa_{RotD100}/Sa_{RotD50}$ ratios, studies of how the orientation of $Sa_{RotD100}$ varies with period for a given ground motion, and guidance for how $Sa_{RotD100}$ design spectra can be developed and used to develop multicomponent ground motions for engineering analysis. It is anticipated that these results will help bridge the gap between the work of seismic hazard analysts, who typically use Sa_{GM} or Sa_{RotD50} values, and engineers, some of whom prefer to work with $Sa_{RotD100}$ response spectra.

ACKNOWLEDGEMENT

This study was sponsored by the Pacific Earthquake Engineering Research Center (PEER) and funded by the California Earthquake Authority, the California Department of Transportation, and the Pacific Gas & Electric Company. Any opinions, findings, and conclusions or recommendations expressed in this material are those of the authors and do not necessarily reflect those of the sponsoring agencies.

REFERENCES

Baker, J. W., and Cornell, C. A. (2006). "Which spectral acceleration are you using?" *Earthquake Spectra*, 22(2), 293-312.

Beyer, K., and Bommer, J. J. (2006). "Relationships between Median Values and between Aleatory Variabilities for Different Definitions of the Horizontal Component of Motion." *Bulletin of the Seismological Society of America*, 96(4A), 1512-1522.

Boore, D. M. (2010). "Orientation-Independent, Nongeometric-Mean Measures of Seismic Intensity from Two Horizontal Components of Motion." *Bulletin of the Seismological Society of America*, 100(4), 1830-1835.

Boore, D. M., Watson-Lamprey, J., and Abrahamson, N. A. (2006). "Orientation-Independent Measures of Ground Motion." *Bulletin of the Seismological Society of America*, 96(4A), 1502–1511.

Chiou, B., Darragh, R., Gregor, N., and Silva, W. (2008). "NGA Project Strong-Motion Database." *Earthquake Spectra*, 24(1), 23–44.

Huang, Y.-N., Whittaker, A. S., and Luco, N. (2008). "Maximum Spectral Demands in the Near-Fault Region." *Earthquake Spectra*, 24(1), 319-341.

Huang, Y.-N., Whittaker, A. S., and Luco, N. (2010). *Maximum Spectral Demand in the United States*. USGS Open File Report xxxx-xxxx, 217p.

NEHRP (2009). *NEHRP Recommended Seismic Provisions for New Buildings and Other Structures*. 406.

Watson-Lamprey, J., and Boore, D. M. (2007). "Beyond SaGMRotI: Conversion to SaArb, SaSN, and SaMaxRot." *Bulletin of the Seismological Society of America*, 97(5), 1511-1524.